ACSNANO

www.acsnano.org

ARTICLE

Efficient Biexciton Interaction in Perovskite Quantum Dots Under Weak and Strong Confinement

Juan A. Castañeda,[†] Gabriel Nagamine,[†] Emre Yassitepe,[‡] Luiz G. Bonato,[‡] Oleksandr Voznyy,[§] Sjoerd Hoogland,[§] Ana F. Nogueira,[‡] Edward H. Sargent,[§] Carlos H. Brito Cruz,[†] and Lazaro A. Padilha*[,†]

[†]Instituto de Fisica "Gleb Wataghin", Universidade Estadual de Campinas, UNICAMP, P.O. Box 6165, 13083-859 Campinas, São Paulo, Brazil

[‡]Instituto de Quimica, Universidade Estadual de Campinas, UNICAMP, P.O. Box 6154, 13084-971 Campinas, São Paulo, Brazil

[§]Department of Electrical and Computer Engineering, University of Toronto, 10 Kings College Road, Toronto, Ontario M5S 3G4, Canada

S *Supporting Information*

ABSTRACT: **Cesium lead halide perovskite quantum dots (PQDs) have emerged as a promising new platform for lighting applications. However, to date, light emitting diodes (LED) based on these materials exhibit limited efficiencies. One hypothesized limiting factor is fast nonradiative multiexciton Auger recombination. Using ultrafast spectroscopic techniques, we investigate multicarrier interaction and recombination mechanisms in cesium lead halide PQDs. By mapping the dependence of the biexciton Auger lifetime and the biexciton binding energy on nanomaterial size and composition, we find unusually strong Coulomb interactions among multiexcitons in PQDs. This results in weakly emissive biexcitons and trions, and accounts for low light emission efficiencies. We observe that, for strong confinement, the biexciton lifetime depends linearly on the PQD volume. This dependence becomes sublinear in the weak confinement regime as the PQD size increases beyond the Bohr radius. We demonstrate that Auger recombination is faster in PQDs compared to CdSe nanoparticles having the same volume, suggesting a stronger Coulombic interaction in the PQDs. We confirm this by demonstrating an increased biexciton binding energy, which reaches a maximum of about 100 meV, fully three times larger than in CdSe quantum dots. The biexciton shift can lead to low-threshold optical gain in these materials. These findings also suggest that materials engineering to reduce Coulombic interaction in cesium lead halide PQDs could improve prospects for high efficiency optoelectronic devices. Core−shell structures, in particular type-II nanostructures, which are known to reduce the bandedge Coulomb interaction in CdSe/CdS, could beneficially be applied to PQDs with the goal of increasing their potential in lighting applications.**

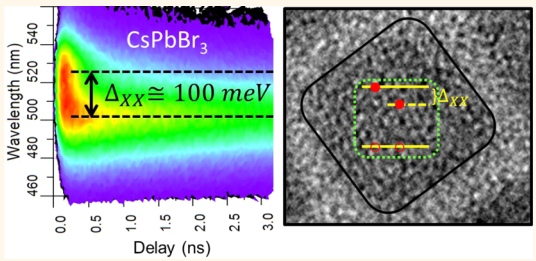

KEYWORDS: *perovskite, quantum dots, ultrafast dynamics, Auger recombination, multiexciton*

The search for novel materials to serve as the platform for optoelectronic devices has intensified in the past decade. The goal is to find structures that will allow for more efficient and environmentally friendly devices. In particular, the search for sources of clean energy has stimulated research on materials and architectures for next-generation solar cells. On the same path, display technologies have demanded higher efficiency LEDs with better color resolution. In this context, hybrid and inorganic lead halide perovskites have emerged as a promising new base material for optoelectronics applications due to their outstanding photophysical and electronic transport properties.[1−5]

Following the results from bulk methylammonium lead halide perovskite materials as the absorption layer in photovoltaic devices,[1−4] the first synthesis of all-inorganic perovskite nanocrystals was reported last year. The Cs-based perovskite nanostructures reported by Protesescu et al. have shown narrow photoluminescence (PL) spectra and high PL quantum efficiency, and a bandgap that can be widely tuned upon the substitution of the halide from Cl to Br and to I.[6,7] These results suggested that Cs-based perovskite nanocrystals could be ideal for lighting applications such as the active layers in LEDs. In fact, a low threshold for amplified spontaneous emission has been recently reported for cesium lead halide perovskite quantum dots, PQDs.[8] Nevertheless, the first reports

Received: June 13, 2016
Accepted: August 30, 2016
Published: August 30, 2016

DOI: 10.1021/acsnano.6b03908
ACS Nano 2016, 10, 8603−8609

for PQD-based LEDs have shown poor performance, with maximum external quantum efficiency, EQE, of about 0.1%.[5,9] The low EQE for the PQD-based LEDs could be a result of multiexciton interactions causing nonradiative decay due to enhanced Auger recombination. In particular trion formation could be an important effect that reduces the EQE in ligh-emitting devices based on nanocrystals.

In a recent work, Makarov et al. reported on the multiexciton interaction in PQDs showing properties distinct from Cd- and Pb-based quantum dots.[10] They showed that multiexciton interactions in PQDs are about 1 order of magnitude stronger than in Cd- and Pb-based nanostructures. Furthermore, the universal volume-scaling of the biexciton Auger lifetime previously observed for spherical nanoparticles of a number of different compositions[11,12] appears not to apply to PQDs.[10] However, the results presented are limited to only few samples (three sizes of $CsPbBr_3$ and only one sample of $CsPbI_3$ PQDs, and another of mixed Br-I), and all of them with large sizes. And, as hypothesized by these authors, the nonvolume scaling of the biexciton lifetime may be explained by the fact that the size of PQDs is comparable or larger than the exciton Bohr radius: in other words, these nanoparticles are far from the strong confinement regime.[10] Conversely, CdSe QDs with diameters as large as 9 nm follow the universal volume scaling, even though their exciton Bohr radius is about 5.6 nm.[13] Consequently, this hypothesis needs to be experimentally verified. Furthermore, single particle spectroscopy at low temperature performed by Rainò et.al. demonstrated very fast PL decay in nonblinking cesium−lead halide PQDs, and emission intensity linearly dependent on the excitation power even at high excitation densities, speculating that these nanostructures are free from Auger recombination and that multiexcitons are highly emissive.[14] Meanwhile, single-particle experiments at room temperature by Park et. al. have demonstrated the presence of fast Auger recombination in PQDs, with low biexciton emission quantum yield.[15]

To seek a clearer understanding of how the quantum confinement influences the multiexciton interaction in this particular class of quantum dots, we investigate, in the present work, the multiexciton interaction in a series of PQDs having various sizes that range from the weak to the strong confinement regime for $CsPbBr_3$ and $CsPbI_3$ PQDs. We do so by mapping not only their dynamics but also their spectral signatures. In agreement with Makarov's recent work,[10] our experimental results indicate a sublinear dependence of the biexciton interaction, including its Auger lifetime, with the volume for $CsPbBr_3$ PQDs with dimensions beyond the Bohr exciton radius ($a_{B,Br} \cong 7$ nm). We show that, for the $CsPbI_3$ and smaller $CsPbBr_3$ PQD samples, the biexciton Auger lifetime follows the same volume scaling (here represented by the absorption cross section at 3.1 eV) observed for other colloidal quantum dots, but, with a much higher Auger rate. For larger PQDs ($d > 7.0$ nm), we observe strong composition dependence for the Auger recombination, which becomes slower for iodide PQDs as compared to bromide ones. Such behavior may be explained by the difference in the confinement regime for both compositions. The strong multiexciton interaction in PQDs is also evidenced from the large biexciton binding energy, which reaches a maximum of about 100 meV, pointing to the promise for low-threshold amplified spontaneous emission in these nanomaterials, consistent with recent report by Yakunin et al.[8]

RESULTS AND DISCUSSION

To map the size- and composition-dependence of multiexciton interaction in these nanomaterials, we synthesized $CsPbBr_3$ PQDs with bandgap energies varying from 2.44 eV (508 nm) to 2.86 eV (434 nm), corresponding to more than 1 order of magnitude change in volume (estimated length of the cubic structure from 3.5 to 13.1 nm). For the $CsPbI_3$ samples, the range of sizes was more modest because very small nanocrystals were unstable. For this case, samples with band gap varying from 1.80 eV (690 nm) to 1.94 eV (640 nm) were synthesized, corresponding to a change in volume by a factor of nearly 5. For comparison, a $CdPbBr_{1.5}I_{1.5}$ PQDs sample was also investigated in these studies. Figure 1 shows examples of the linear absorption and photoluminescence spectra for some of the investigated samples together with one TEM image. Other examples of TEM images for the studied samples are shown in Figure S1. For the investigated samples, the Stokes shift is estimated to be about 80 meV, this value tends to increase to nearly 100 meV for smaller nanoparticles.

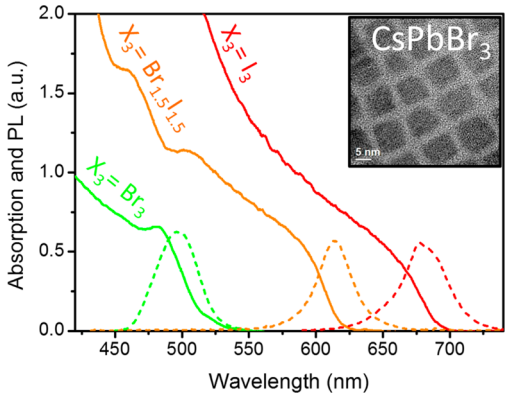

Figure 1. Examples of absorption and photoluminescence spectra for $CsPbX_3$ PQDs samples. The inset shows, as an example, one of the TEM images for the $CsPbBr_3$ PQDs sample.

To measure the multiexciton dynamics, we performed ultrafast transient absorption experiments for which the excitation was selected at 3.1 eV and the probe was selected near the first absorption peak. For each sample, the pump intensity was varied by more than 1 order of magnitude, from a density of $\langle N \rangle \cong 0.1$ to $\langle N \rangle \geq 5.0$ photons absorbed per PQD. Figure 2 shows an example of the measured transient absorption for a $CsPbI_3$ sample, for which a fast decay component of about 100 ps emerges as the pump intensity increases. In order to ascertain whether the 100 ps decay component is from biexcitons, and rule out the influence of trions, we have used Poisson statistics to analyze our results at early times (before Auger recombination eliminates the multiexcitons) and for long delays, when only single excitons are left in the PQD. If we let the number of absorbed photons per PQD, $\langle N \rangle = \langle N \rangle_{Photons} \sigma_{3.1eV}$ (where $\langle N \rangle_{Photons}$ is the average number of photons, per area, per excitation pulse and $\sigma_{3.1eV}$ is the absorption cross section measured at 3.1 eV), follow Poisson statistics, then once 500 ps have elapsed, due to Auger recombination for multiple excitons, each excited PQD is expected to be left with only one exciton (see SI for details). From this starting point we then fit the long delay magnitude (B, measured at 500 ps) as a function of the density of photons per pulse by $B = B_0(1 - \exp(-\langle N \rangle_{Photons} \sigma_{3.1eV}))$, where B_0 is the B saturation magnitude. We also fit the magnitude of the fast

DOI: 10.1021/acsnano.6b03908
ACS Nano 2016, 10, 8603−8609

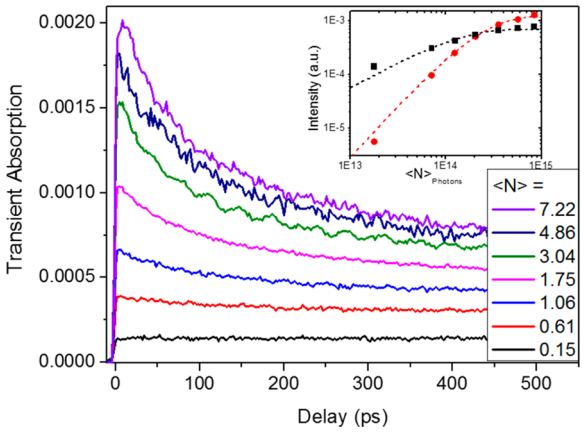

Figure 2. Transient absorption measurement for $CsPbI_3$ PQDs with absorption at 670 nm (emission at 690 nm). The data show the fast component emerging due to the Auger recombination of biexcitons. The inset shows the dependence on the pump intensity of the long delay amplitude (black squares) and of the fast component amplitude (red circles) fit to the Poisson distribution to the single exciton and biexciton population, respectively. $\langle N\rangle_{Photons}$ is the number of photons per pulse per cm^2 and $\langle N\rangle = \langle N\rangle_{Photons}\sigma_{3.1eV}$ is the average number of photons absorbed per PQD.

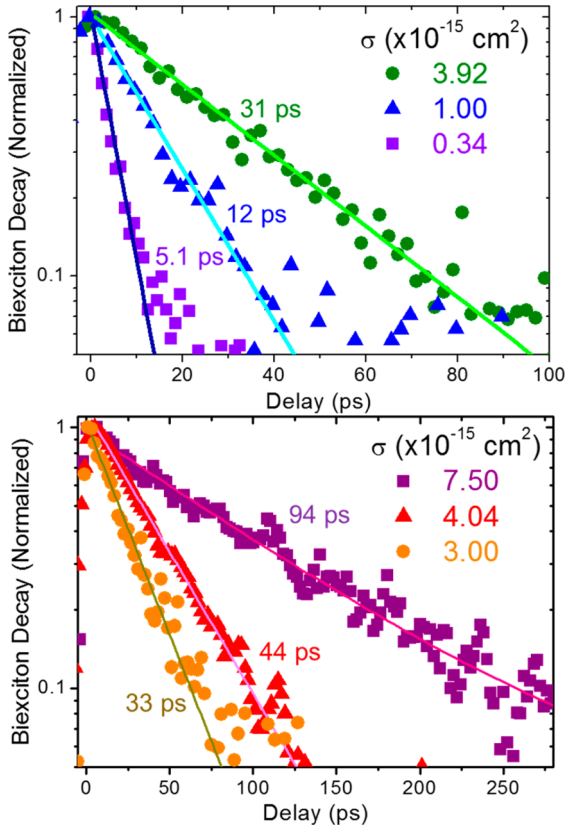

Figure 3. Biexciton dynamics for three samples of (a) $CsPbBr_3$ PQDs and (b) $CsPbI_3$ PQDs showing the size dependence of the Auger recombination lifetime. To isolate the biexciton dynamics we subtract the contribution from the single exciton obtained from the lowest pump intensity scan, $\langle N\rangle \leq 0.2$.

component which corresponds to an absorption bleach in the PQDs with at least two excitons: $A = A_0(1 - \exp(-\langle N\rangle_{Photons}\sigma_{3.1eV})(1 + \langle N\rangle_{Photons}\sigma_{3.1eV}))$. When the fast component originates exclusively from biexcitons, the Poisson statistics described above should fit the excitation dependence of A and B using the same value for $\sigma_{3.1eV}$. The inset in Figure 2a shows both fittings for the early and late times, resulting in $\sigma_{3.1eV} = (7.5 \pm 0.8) \times 10^{-15}cm^2$.

To calculate $\sigma_{3.1eV}$, we have also measured the pump dependence of the transient photoluminescence using a time-correlated single photon counting (TCSPC) system with resolution of about 100 ps. For this experiment, excitation was chosen at either 3.1 eV (for the bromide and some of the iodide samples) or 2.3 eV (for most of the iodide samples) in order to minimize the influence of possible photoionization. The details are provided in full in Figure S3 in the SI.

Size Dependence of Auger Recombination. Figure 3a,b shows the multiexciton dynamics for a series of $CsPbBr_3$ (Figure 3a) and $CsPbI_3$ (Figure 3b). In order to isolate the contribution from the multiexcitons dynamics on the high intensity scans, we subtract the single exciton contribution obtained from the lowest intensity scan (typically, for intensities such as $\langle N\rangle \approx 0.1$), for which multi photon absorption, and the consequent multiexciton generation, is negligible. From those results, we can see that for more than 90% of the signal the dynamics follow a monoexponential decay, indicating that only a small fraction of the sample may have trion formation. We conclude that the presence of trions will influence the results by less than 10%. For some samples, at high excitation flux ($\langle N\rangle \geq 5.0$) we observe an increased influence of a slower decay mechanism, which is suggestive of further trion formation (see Figure S4 in the SI). In contrast to our findings, Makarov et al. have found substantial trion formation.[10] In their experiments, the excitation was chosen at 3.6 eV, higher than the 3.1 eV used in this current work. For lead chalcogenide quantum dots, it has been shown that the higher the exciting photon energy, the higher the probability of photoionization.[16] Assuming that photoionization occurs as a tunneling process as described in refs 16 and 17, we expect the same trend to be true for PQDs, explaining the difference observed in the dynamics. From Figure 3a,b, it can be seen that the biexciton Auger recombination is faster for smaller PQDs.

To understand the size influence on the biexciton dynamics, we compare the biexciton Auger lifetime for all samples as a function of the nanoparticle cross section as shown in Figure 4. We have found that the size distribution for some of the smaller PQDs, as measured using TEM, was too large to obtain a meaningful nanoparticle size, in view of limited-quality TEM images acquired from these samples. Therefore, we chose to use the absorption cross section at 3.1 eV ($\sigma_{3.1eV}$) instead of the volume measured by the TEM, as a measure of the nanomaterial size. Because of size inhomogeneity and possibly agglomeration of PQDs on the TEM grid, it is possible that the average size of the PQDs observed in the TEM images does not correspond to the average size of the samples probed using transient absorption and transient PL experiments, as previously observed in PbSe nanorods.[18] For the samples from which we were able to obtain high quality TEM images, we observe a linear trend between volume and $\sigma_{3.1eV}$ (see Figure S2). Consequently, plotting the biexciton Auger lifetime as a function of $\sigma_{3.1eV}$ reflects its volume dependence. As can be seen in Figure 4, the results obtained here agree with the previously reported by Makarov et al., showing that for large bromide PQDs, the biexciton decay depends sublinearly on the PQD volume.[10] Fitting the power dependence for the largest

DOI: 10.1021/acsnano.6b03908
ACS Nano 2016, 10, 8603−8609

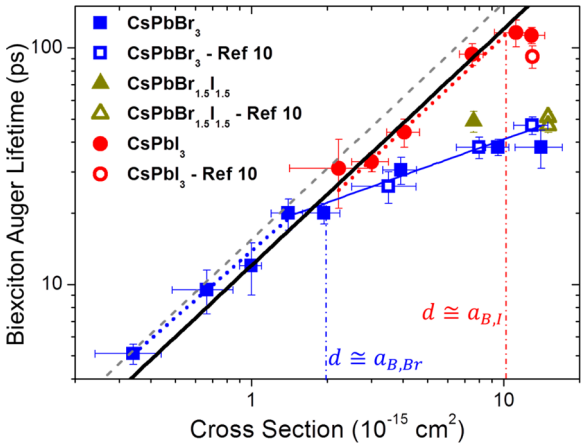

Figure 4. Biexciton Auger lifetime as a function of the absorption cross section at 3.1 eV for $CsPbBr_3$, $CsPbI_3$, and $CsPbBr_{1.5}I_{1.5}$ PQDs. The open symbols are data from ref 10. The full blue line is the sublinear fit to the $CsPbBr_3$data for samples with cross section above $\sigma_{3.1eV} = 2 \times 10^{-15}$ cm^2. The dotted blue and red lines are power dependence fit to the smallest $CsPbBr_3$ and $CsPbI_3$, respectively, showing nearly linear dependence, which is shown in the full black line. The dashed gray line is the biexciton lifetime dependence with $\sigma_{3.1eV}$ for CdSe quantum dots.[20,21]

bromide PQDs, we obtain $\tau_{XX} \propto V^{(0.38\pm0.04)}$, which is close to a linear dependence with the nanoparticle edge length. In fact, if we consider only the very large samples, the biexciton Auger lifetime appears to saturate at around 40−50 ps. This behavior is distinct for spherical or for cubic nanoparticles; however, a similar subvolumetric dependence of the Auger lifetime has been previously observed in PbSe and CdSe nanorods.[18,19] In those cases, this behavior has been attributed to a bimolecular Auger interaction, a two-body process in which each exciton is formed in a different portion of the nanomaterial.[19] The reason for such behavior in PQDs could be the weak confinement regime for nanomaterials in which the edge length d is larger than the exciton Bohr radius. This hypothesis can be verified if we consider only bromide PQDs with $\sigma_{3.1eV} \leq 2 \times 10^{-15}$ cm^2. In this case, the dependence with volume follows $\tau_{XX} \propto V^{(0.93\pm0.06)}$, approaching the linear dependence observed for CdSe or PbSe quantum dots. It is interesting to point out that, according to the fitting for volume vs $\sigma_{3.1eV}$ in Figure S2, $\sigma_{3.1eV} = 2 \times 10^{-15}$ cm^2 corresponds to $CsPbBr_3$ PQDs with average edge length of $d \cong 7.1$ nm, which is close to the expected exciton Bohr radius for $CsPbBr_3$.[6] Iodide PQDs have a larger exciton Bohr radius ($a_{B,I} \cong 12$ nm),[6] and the strong confinement regime can be achieved at larger PQDs sizes. In fact, for most of the $CsPbI_3$ measured samples, Auger lifetime scales linearly with the cross section (volume). Only for the sample with the largest iodide nanomaterials, the linear trend appears not to be valid. Fitting only the data for the iodide samples in Figure 4, we obtain $\tau_{XX} \propto V^{(0.99\pm0.08)}$.

From our data, it can be noted that for larger PQDs, there is a dependence of the biexciton dynamics on nanomaterial composition. We observe that the composition dependence of τ_{XX} vanishes for small sizes and, to a good approximation, we can fit the dependence of τ_{XX} on $\sigma_{3.1eV}$ with one single linear fit for all iodide samples and all the bromide ones with $\sigma_{3.1eV} \leq 2 \times 10^{-15}$ cm^2 (black line in Figure 4). Continuing our analysis, considering the data from ref 10 for the iodide PQD, together with the largest iodide sample measured here, we find that the dependence of the τ_{XX} on the absorption cross section becomes sublinear for nanomaterials with $\sigma_{3.1eV} \approx 10 \times 10^{-15}$ cm^2. This corresponds to an edge length of $d \cong 12.2$ nm, which agrees well with the exciton Bohr radius of iodide perovskites, $a_{B,I} \cong 12$ nm.[6] This reinforces that the sublinear behavior is the result solely from the weak confinement regime. Finally, we have measured one size of the mixed $CdPbBr_{1.5}I_{1.5}$ PQDs which results in the same biexciton lifetime as was measured in ref 10. This suggests that mixed halide PQDs also exhibit sublinear dependence of the biexciton lifetime in the weak confinement regime. Assuming the same volume dependence of τ_{XX} for the mixed-halide PQDs as for the iodide and bromide, we find the threshold for the sublinear dependence to be $\sigma_{3.1eV} \approx 4 \times 10^{-15}$ cm^2. This corresponds to $d \cong 9.0$ nm, which is close to the expected exciton Bohr radius for the mixed halide PQDs of $a_{B,BrI} \cong 9.5$ nm. However, at this point, this assumption is merely speculative and more data would be necessary to verify it. The change on size dependence for τ_{XX} observed for PQDs when moving from strong to the weak confinement regime is more pronounced than in other nanomaterials, such as CdSe QDs, for which the universal volume-scaling is observed up to 9 nm diameters[11] despite entering the weak confinement regime ($a_{B,CdSe} \cong 5.6$ nm).

In accordance with what was previously observed,[10] when compared to CdSe or PbSe quantum dots, and comparing similar volumes, we find that PQDs have a much stronger multiexciton interaction, resulting in τ_{XX} about 1 order of magnitude faster. When comparing the relation between $\sigma_{3.1eV}$ and the volume for PQDs and CdSe QDs, it has been seen that the cross section for CdSe is also nearly 1 order of magnitude larger than for PQDs with the same volume. When comparing the biexciton Auger lifetime for PQDs and CdSe as a function of $\sigma_{3.1eV}$, we find a surprisingly good agreement (gray dashed line in Figure 4 represents the dependence for CdSe quantum dots and it is taken from the best fit of the data from ref 20). Consequently, the data show that, in the strong confinement regime, the dependence of the Auger recombination on the absorption cross section in PQDs is the same as in CdSe quantum dots whose volume is about five times larger. In other words, we suggest that, in cesium lead halide PQDs, differently form other QDs structures, the excitons are generated in an effective excitonic volume that is much smaller than their actual volume.

The efficient Auger interaction observed in this class of materials results in weakly emitting multiexcitons. In fact, taking into account the PL lifetime measured for the bromide (from about 4.6 to 6.3 ns) and for iodide (from 10 to 13 ns) PQDs, we can estimate the biexciton PL quantum efficiency by $QY_{XX} = 4\frac{\tau_{XX}}{\tau_{PL}}QY_X$. From our ensemble measurements, we obtain for all $CsPbBr_3$ samples $\frac{QY_{XX}}{QY_X} \leq 0.02$, while for the $CsPbI_3$ samples $\frac{QY_{XX}}{QY_X} \leq 0.04$. These numbers are in agreement with recent results from single particle spectroscopy which indicated a maximum ratio between QY_{XX} and QY_X of about 6%, which is achieved for iodide samples.[15] On the other hand, our results contradict the recent low-temperature single particle studies that suggests that multiexcitons are highly emissive in bromide PQDs.[14] The PL lifetime measured at low temperature in ref 14 is close to the value obtained due to the presence of ionized samples in our ensemble measurements for bromide PQDs with similar average sizes.

Biexciton Binding Energy. On the basis of the strong biexciton interaction observed in the dynamics, we further

DOI: 10.1021/acsnano.6b03908
ACS Nano 2016, 10, 8603−8609

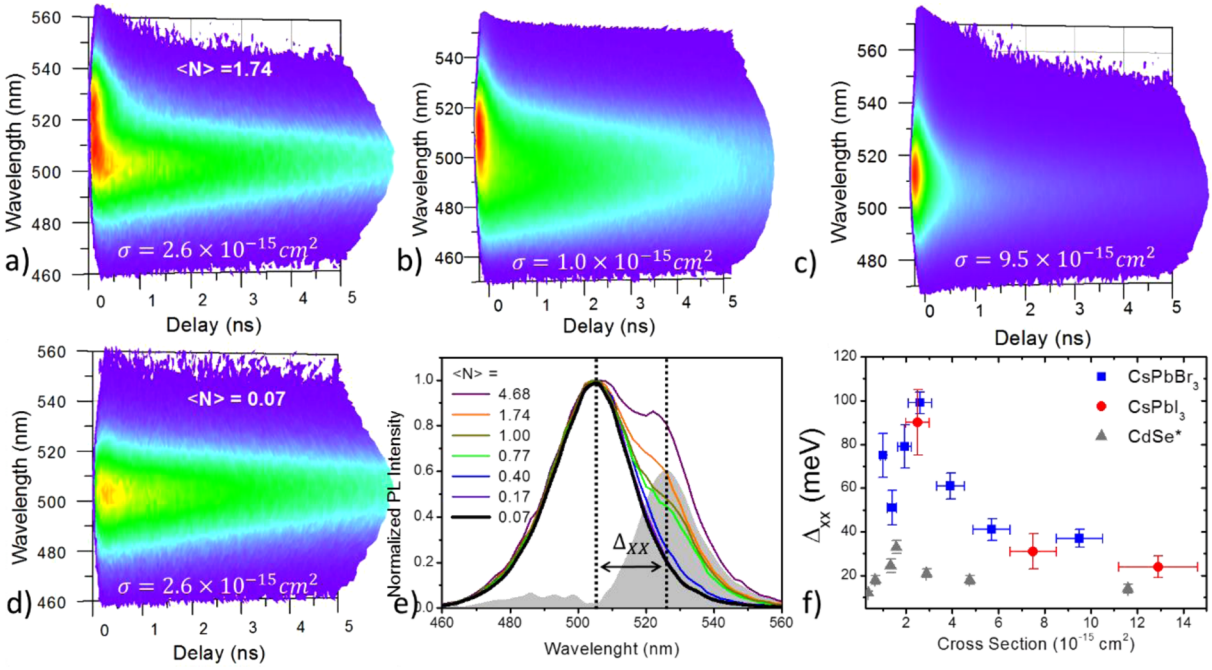

Figure 5. Temporally and spectrally resolved photoluminescence at high excitation density measured for three samples of $CsPbBr_3$ PQDs (a, b, and c). A scan at low excitation density for the same sample in (a) is shown in (d). The intensity in panels a, b, c, and d, is plotted in log-scale. The biexciton binding is extracted from the difference between the high and low excitation density at the short delay spectra (~100 ps) as shown by the shaded area in (e). In (f), we show the size dependence of the biexciton binding energy for $CsPbBr_3$ and $CsPbI_3$ PQDs. The biexciton binding energy data for CdSe is taken from ref 21 and plotted versus the cross section with the cross section calculated from ref 20.

investigated the strength of the multiexciton interaction in PQDs by measuring the biexciton interaction energy, Δ_{XX}. This can be obtained in the multiexciton regime from the spectral shift of the photoluminescence in time. We have collected the temporal and spectrally resolved photoluminescence at low excitation levels with only single excitons present, and at high excitation levels (typically, $\langle N \rangle \cong 2$), to warrant the presence of biexcitons. As shown in Figure 5a–d, we resolve the biexciton shift, which emerges as a signal convolved with the system response of about 100 ps. The size dependence of the biexciton shift is evident when we compare Figure 5a–c for bromide PQDs with different cross sections. To calculate Δ_{XX}, we decompose the zero delay PL signal on the contribution from the biexciton and the single exciton extracted from the low excitation density scan (Figure 5d), and from the long delay of the high energy scan, as it is shown by the shaded area in Figure 5e. The summary of the measured biexciton binding energy for several sizes is shown in Figure 5f. As the PQDs gets smaller, Δ_{XX} increases, approaching 100 meV for iodide and bromide PQDs. This shift is about three times larger than the maximum shift observed for CdSe QDs,[21] confirming our results from the time-resolved experiments that indicates strong Coulomb interactions in PQDs. Our results suggest that Δ_{XX} reaches the maximum value for bromide PQDs when $\sigma_{3.1eV} \cong 2 \times 10^{-15}$ cm^2. For smaller sizes, we observe a small reduction on the biexciton shift. It is interesting to point out that the maximum value for the biexciton binding energy for bromide PQDs is achieved at similar sizes for which we observe the changing from the weak to the strong confinement regime (Figure 4). Similar trends have been observed for CdSe QDs[21] and were assigned to the repulsive Coulomb electron–electron and hole–hole interactions, which increases in the smaller sizes.[21] In the current work, the saturation of the biexciton binding energy is reached at significantly larger sizes (~7 nm for bromide PQDs compared to ~3 nm for CdSe[21]), reinforcing that the Coulombic interaction in perovskites is stronger than in CdSe QDs. Strong biexciton interaction, similar to the one found in PQDs, has been previously observed from optical gain experiments in organic–inorganic hybrid perovskite quantum-wells.[22] In fact, the large biexciton binding energy observed for PQDs is expected to reduce the threshold for amplified stimulated emission, as recently reported by Yakunin et al.[8] Nanomaterial band engineering aiming to reduce Auger recombination without reducing the binding energy, as shown for CdSe/CdS core/shell heterostructures, if successfully applied to PQDs, can make these nanostructures a promising material for lasing applications, in particular, electrically pumped QD-based lasers.

The three largest bromide PQDs samples shown in Figure 5f have a clear trend of reducing the biexciton binding energy with the increased cross section. It is interesting to note that the two largest PQDs, which are on the weak confinement regime, have similar biexciton shift, Δ_{XX} = 40 meV. This value is close to the biexciton binding energy measured for $CsPbBr_3$ nanowires in the weak confinement regime[23] and it approaches the exciton binding energy for bulk $CsPbBr_3$.[6] However, it is still larger than the biexciton binding energy expected for bulk $CsPbBr_3$, which is below 10 meV.[23] Following the same trend, for the iodide samples, we would expect that for those nanoparticles the limit for the biexciton binding energy would be close to 20 meV, the expected bulk value for the exciton binding energy. Indeed, the biexciton binding energy measured for the iodide PQD in the weak confinement regime is 23 meV, close to the expected value. A similar trend has been previously observed in CdSe QDs in the weak confinement regime, where Δ_{XX} would approach the bulk exciton binding energy rather than the biexciton binding energy.[21]

DOI: 10.1021/acsnano.6b03908
ACS Nano 2016, 10, 8603–8609

These results, all taken together, indicate that, in cesium lead halide perovskites nanoparticles, the Coulomb interaction is stronger than in other semiconductor nanostructures. This could favor Coulomb assisted processes, in particular, impact ionization, resulting in high-efficiency carrier multiplication (CM).[24−26] Nevertheless, recent results from Makarov et al. have shown that no CM can be measured in PQDs for photon energy below $2.65E_g$, which is similar to the behavior already observed in other nanomaterials.[10] This suggests that CM is not enhanced in PQDs despite the increased Coulomb interaction at the band edge. The opposite behavior has been observed in PbSe nanorods, for which the Auger recombination is slower than PbSe quantum dots, but the CM efficiency is enhanced compared to the spherical nanoparticles.[18,27] This behavior has been explained based on the interplay between the bimolecular Auger behavior[19] and on the predicted enhanced Coulomb screening in nanorods at high energy levels.[28] The results observed for PQDs cannot be explained by those arguments, suggesting the need for further experimental and theoretical analysis to completely understand the peculiar multiexciton interaction in PQDs. According to the model of competing decay channels proposed by Stewart et al.,[24] stronger Coulomb interaction should decrease the electron−hole pair creation energy, and this will affect the CM *slope* more than the *threshold*. Consequently, in order to determine whether CM is influenced by strong Auger recombination in PQDs, CM studies need to be performed at higher photon energy, that is, for $\hbar\omega \geq 3E_g$.

CONCLUSIONS

In conclusion, this work describes how quantum confinement influences the multiexciton interaction in cesium−lead halide perovskite by investigating quantum dots with more than 1 order of magnitude variation in volume. When compared to CdSe quantum dots, the biexciton Auger lifetime in PQDs is nearly 1 order of magnitude faster than their CdSe counterparts with similar volume.[10] However, when compared in terms of the absorption cross section, we find a surprisingly good agreement on the biexciton lifetime for both materials at the strong confinement regime. This suggests that, in PQDs, the exciton and the biexciton experience an excitonic volume smaller than the actual physical volume. Furthermore, we have shown that the sublinear dependence of Auger lifetime with volume is the result of the weak confinement regime and that the linear dependence is reached as the nanoparticles are smaller than the exciton Bohr radius. The strong multiexciton interaction and its dependence on the PQD volume are also observed in the biexciton binding energy, which reaches values of about 100 meV, which is three times higher than the maximum observed in CdSe quantum dots.[21] The large biexciton shift observed in PQDs could favor low-threshold amplified stimulated emission at those wavelengths, turning those materials interesting for lasing applications. On the other hand, the fast Auger recombination results in poorly emissive multiexcitons, which is detrimental to PQD-based lighting devices such as LEDs. Further studies to better comprehend the multiexciton interaction and to engineer novel perovskite based heteronanostructures, such as type-II core−shell, with controlled Auger recombination, are necessary in order to pursue highly efficient optoelectronic devices based on PQDs.

METHODS

Sample Preparation. Samples investigated in this work were synthesized following Protesescu et al.[6] In brief, the reaction is carried out in two steps: first, by solubilizing $PbBr_2$ and/or PbI_2 in oleic acid and oleylamine, with 1-octadecene as a noncoordinating solvent; second, the previously prepared cesium oleate solution is injected to PbX_2 mixture at temperatures between (140−200 °C) resulting in perovskite quantum dots. For all spectroscopic measurements, the samples were dispersed in hexane and loaded in sealed 1 mm spectroscopy grade quartz cuvettes. For all samples, the concentrations were adjusted to have an optical density at the first absorption peak of about 0.2. Sample degradation during the optical experiments was ruled out by measuring the absorption and PL before and after the experiments. The samples investigated in this work have shown imperceptible changes during the experiment, indicating that they were stable over the duration of the experiments.

ASSOCIATED CONTENT

Supporting Information

The Supporting Information is available free of charge on the ACS Publications website at DOI: 10.1021/acsnano.6b03908.

Experimental details of PQD synthesis, transient photoluminescence measurements to obtain the absorption cross section, and a brief discussion on the influence of trions on our measurements. (PDF)

AUTHOR INFORMATION

Corresponding Author

*E-mail: padilha@ifi.unicamp.br.

Notes

The authors declare no competing financial interest.

ACKNOWLEDGMENTS

This publication is based in part on work supported by the Ontario Research Fund—Research Excellence Program, and by the Natural Sciences and Engineering Research Council (NSERC) of Canada. E.Y. acknowledges support from FAPESP (2014/18327-9 and 2013/05798-0) fellowship. J.A.C., G.N., C.H.B.C., and L.A.P. acknowledge the financial support from FAPESP (2013/16911-2). A.F.N. acknowledges FAPESP (2014/21928-4), CNPq, and INEO. JAC and GN acknowledges the scholarship from CAPES, and EY acknowledges LNano-CNPEM (TEM-19813) for high resolution transmission microscopy facility.

REFERENCES

(1) Kojima, A.; Teshima, K.; Shirai, Y.; Miyasaka, T. Organometal Halide Perovskites as Visible-Light Sensitizers for Photovoltaic Cells. *J. Am. Chem. Soc.* **2009**, *131*, 6050−6051.

(2) Liu, M.; Johnston, M. B.; Snaith, H. J. Efficient Planar Heterojunction Perovskite Solar Cells by Vapour Deposition. *Nature* **2013**, *501*, 395−398.

(3) Burschka, J.; Pellet, N.; Moon, S.-J.; Humphry-Baker, R.; Gao, P.; Nazeeruddin, M. K.; Gratzel, M. Sequential Deposition as a Route to High-Performance Perovskite-Sensitized Solar Cells. *Nature* **2013**, *499*, 316−319.

(4) Jeon, N. J.; Noh, J. H.; Kim, Y. C.; Yang, W. S.; Ryu, S.; Seok, S. I. Solvent Engineering for High-Performance Inorganic−Organic Hybrid Perovskite Solar Cells. *Nat. Mater.* **2014**, *13*, 897−903.

(5) Zhang, X.; Lin, H.; Huang, H.; Reckmeier, C.; Zhang, Y.; Choy, W. C. H.; Rogach, A. L. Enhancing the Brightness of Cesium Lead Halide Perovskite Nanocrystal Based Green Light-Emitting Devices through the Interface Engineering with Perfluorinated Ionomer. *Nano Lett.* **2016**, *16*, 1415−1420.

DOI: 10.1021/acsnano.6b03908
ACS Nano 2016, 10, 8603−8609

(6) Protesescu, L.; Yakunin, S.; Bodnarchuk, M. I.; Krieg, F.; Caputo, R.; Hendon, C. H.; Yang, R. X.; Walsh, A.; Kovalenko, M. V. Nanocrystals of Cesium Lead Halide Perovskites ($CsPbX_3$, X = Cl, Br, and I): Novel Optoelectronic Materials Showing Bright Emission with Wide Color Gamut. *Nano Lett.* **2015**, *15*, 3692−3696.
(7) Nedelcu, G.; Protesescu, L.; Yakunin, S.; Bodnarchuk, M. I.; Grotevent, M. J.; Kovalenko, M. V. Fast Anion-Exchange in Highly Luminescent Nanocrystals of Cesium Lead Halide Perovskites ($CsPbX_3$, X = Cl, Br, I). *Nano Lett.* **2015**, *15*, 5635−5640.
(8) Yakunin, S.; Protesescu, L.; Krieg, F.; Bodnarchuk, M. I.; Nedelcu, G.; Humer, M.; De Luca, G.; Fiebig, M.; Heiss, W.; Kovalenko, M. V. Low-Threshold Amplified Spontaneous Emission and Lasing from Colloidal Nanocrystals of Caesium Lead Halide Perovskites. *Nat. Commun.* **2015**, *6*, 8056.
(9) Li, X.; Wu, Y.; Zhang, S.; Cai, B.; Gu, Y.; Song, J.; Zeng, H. CsPbX3 Quantum Dots for Lighting and Displays: Room-Temperature Synthesis, Photoluminescence Superiorities, Underlying Origins and White Light-Emitting Diodes. *Adv. Funct. Mater.* **2016**, *26*, 2435−2445.
(10) Makarov, N. S.; Guo, S.; Isaienko, O.; Liu, W.; Robel, I.; Klimov, V. I. Spectral and Dynamical Properties of Single Excitons, Biexcitons, and Trions in Cesium−Lead-Halide Perovskite Quantum Dots. *Nano Lett.* **2016**, *16*, 2349−2362.
(11) Robel, I.; Gresback, R.; Kortshagen, U.; Schaller, R. D.; Klimov, V. I. Universal Size-Dependent Trend in Auger Recombination in Direct-Gap and Indirect-Gap Semiconductor Nanocrystals. *Phys. Rev. Lett.* **2009**, *102*, 177404.
(12) Robel, I.; Gresback, R.; Kortshagen, U.; Schaller, R. D.; Klimov, V. I. Universal Size-Dependent Trend in Auger Recombination in Direct-Gap and Indirect-Gap Semiconductor Nanocrystals. *Phys. Rev. Lett.* **2009**, *102*, 177404.
(13) Meulenberg, R. W.; Lee, J. R. I.; Wolcott, A.; Zhang, J. Z.; Terminello, L. J.; van Buuren, T. Determination of the Exciton Binding Energy in CdSe Quantum Dots. *ACS Nano* **2009**, *3*, 325−330.
(14) Rainò, G.; Nedelcu, G.; Protesescu, L.; Bodnarchuk, M. I.; Kovalenko, M. V.; Mahrt, R. F.; Stöferle, T. Single Cesium Lead Halide Perovskite Nanocrystals at Low Temperature: Fast Single-Photon Emission, Reduced Blinking, and Exciton Fine Structure. *ACS Nano* **2016**, *10*, 2485−2490.
(15) Park, Y.-S.; Guo, S.; Makarov, N. S.; Klimov, V. I. Room Temperature Single-Photon Emission from Individual Perovskite Quantum Dots. *ACS Nano* **2015**, *9*, 10386−10393.
(16) Padilha, L. A.; Robel, I.; Lee, D. C.; Nagpal, P.; Pietryga, J. M.; Klimov, V. I. Spectral Dependence of Nanocrystal Photoionization Probability: The Role of Hot-Carrier Transfer. *ACS Nano* **2011**, *5*, 5045−5055.
(17) McGuire, J. A.; Sykora, M.; Robel, I. n.; Padilha, L. A.; Joo, J.; Pietryga, J. M.; Klimov, V. I. Spectroscopic Signatures of Photocharging due to Hot-Carrier Transfer in Solutions of Semiconductor Nanocrystals under Low-Intensity Ultraviolet Excitation. *ACS Nano* **2010**, *4*, 6087−6097.
(18) Padilha, L. A.; Stewart, J. T.; Sandberg, R. L.; Bae, W. K.; Koh, W.-K.; Pietryga, J. M.; Klimov, V. I. Aspect Ratio Dependence of Auger Recombination and Carrier Multiplication in PbSe Nanorods. *Nano Lett.* **2013**, *13*, 1092−1099.
(19) Htoon, H.; Hollingsworth, J. A.; Dickerson, R.; Klimov, V. I. Effect of Zero- to One-Dimensional Transformation on Multiparticle Auger Recombination in Semiconductor Quantum Rods. *Phys. Rev. Lett.* **2003**, *91*, 227401.
(20) Nanda, J.; Ivanov, S. A.; Htoon, H.; Bezel, I.; Piryatinski, A.; Tretiak, S.; Klimov, V. I. Absorption Cross Sections and Auger Recombination Lifetimes in Inverted Core-Shell Nanocrystals: Implications for Lasing Performance. *J. Appl. Phys.* **2006**, *99*, 034309.
(21) Achermann, M.; Hollingsworth, J. A.; Klimov, V. I. Multiexcitons Confined within a Subexcitonic Volume: Spectroscopic and Dynamical Signatures of Neutral and Charged Biexcitons in Ultrasmall Semiconductor Nanocrystals. *Phys. Rev. B: Condens. Matter Mater. Phys.* **2003**, *68*, 245302.
(22) Kato, Y.; Ichii, D.; Ohashi, K.; Kunugita, H.; Ema, K.; Tanaka, K.; Takahashi, T.; Kondo, T. Extremely Large Binding Energy of Biexcitons in an Organic−Inorganic Quantum-Well Material $(C_4H_9NH_3)_2PbBr_4$. *Solid State Commun.* **2003**, *128*, 15−18.
(23) Eaton, S. W.; Lai, M.; Gibson, N. A.; Wong, A. B.; Dou, L.; Ma, J.; Wang, L.-W.; Leone, S. R.; Yang, P. Lasing in Robust Cesium Lead Halide Perovskite Nanowires. *Proc. Natl. Acad. Sci. U. S. A.* **2016**, *113*, 1993−1998.
(24) Stewart, J. T.; Padilha, L. A.; Bae, W. K.; Koh, W.-K.; Pietryga, J. M.; Klimov, V. I. Carrier Multiplication in Quantum Dots within the Framework of Two Competing Energy Relaxation Mechanisms. *J. Phys. Chem. Lett.* **2013**, *4*, 2061−2068.
(25) Nozik, A. J. Quantum Dot Solar Cells. *Phys. E* **2002**, *14*, 115−120.
(26) Padilha, L. A.; Stewart, J. T.; Sandberg, R. L.; Bae, W. K.; Koh, W.-K.; Pietryga, J. M.; Klimov, V. I. Carrier Multiplication in Semiconductor Nanocrystals: Influence of Size, Shape, and Composition. *Acc. Chem. Res.* **2013**, *46*, 1261−1269.
(27) Sandberg, R. L.; Padilha, L. A.; Qazilbash, M. M.; Bae, W. K.; Schaller, R. D.; Pietryga, J. M.; Stevens, M. J.; Baek, B.; Nam, S. W.; Klimov, V. I. Multiexciton Dynamics in Infrared-Emitting Colloidal Nanostructures Probed by a Superconducting Nanowire Single-Photon Detector. *ACS Nano* **2012**, *6*, 9532−9540.
(28) Bartnik, A. C.; Efros, A. L.; Koh, W. K.; Murray, C. B.; Wise, F. W. Electronic States and Optical Properties of PbSe Nanorods and Nanowires. *Phys. Rev. B: Condens. Matter Mater. Phys.* **2010**, *82*, 195313.

DOI: 10.1021/acsnano.6b03908
ACS Nano 2016, 10, 8603−8609